International Journal of Pharmaceutical and Bio-Medical Science

ISSN(print): 2767-827X, ISSN(online): 2767-830X

Volume 04 Issue 12 December 2024

Page No : 1046-1067

DOI: https://doi.org/10.47191/ijpbms/v4-i12-20, Impact Factor:7.792

Hematological and Histological Effects Of Pesticide Mixtures in Postpartum and Non-Postpartum Female Wistar Rats

Oghenevwaire, OF[1], Adeyemi, O*[2]

[1,2] Department of Environmental Management and Toxicology, Federal University of Petroleum Resources, PMB 1221, Effurun, Delta State, Nigeria.

ABSTRACT

This study investigated the hematological and histopathological impacts of pesticide mixtures—dichlorvos, dimethoate, and cypermethrin—on postpartum and non-postpartum female Wistar albino rats. A total of 64 female rats were divided into eight groups (A–H), each exposed to specific pesticide combinations over 28 days. Groups B, C, and D received individual pesticides, while Groups E–H were exposed to mixtures, simulating environmental pesticide exposure scenarios. Hematological analysis revealed significant reductions in red blood cell counts (RBC) and hemoglobin (HB) levels, with Group B (dichlorvos) showing the most pronounced decreases (RBC: 7.25 ± 0.19 × 10^6/mm^3; HB: 11.31 ± 0.30 g/dL). Platelet counts were elevated in exposed groups, notably Group F (dichlorvos + cypermethrin: 293.16 ± 4.09 × 10^3/mm^3). Postpartum rats demonstrated enhanced resilience, maintaining higher RBC and HB levels compared to non-postpartum counterparts across all groups. Histopathological examination of the uterus and ovaries revealed extensive damage in pesticide-exposed groups. Uterine tissues exhibited ulcerations, stromal degeneration, and inflammatory infiltration, with Group H (dichlorvos + dimethoate + cypermethrin) showing severe ulceration and stromal infiltration. Ovarian tissues presented with follicular degeneration and stromal congestion, most severe in Group H, where only one viable follicle was observed. These findings highlight the compounded toxic effects of pesticide mixtures, with postpartum physiology providing partial protective adaptations. The study underscores the need for stringent regulation of pesticide use and further exploration of physiological mechanisms mitigating toxicity in reproductive contexts.

KEYWORDS: Pesticide toxicity; Hematological changes; Histopathology; Postpartum resilience; Female Wistar rats

ARTICLE DETAILS

Published On:
31/12/2024

Available on:
https://ijpbms.com/

INTRODUCTION

Pesticides are integral to modern agriculture, enhancing crop yields and controlling pests. However, their extensive use has raised significant concerns regarding potential health risks to non-target organisms, including humans and wildlife. Among these chemicals, dichlorvos, dimethoate, and cypermethrin are commonly employed due to their effectiveness in pest control. Dichlorvos, an organophosphate, functions by inhibiting acetylcholinesterase, leading to the accumulation of acetylcholine and subsequent neurotoxicity (Celik et al., 2009). Dimethoate, another organophosphate, shares a similar mechanism of action, disrupting neural transmission in pests (Kumar et al., 2010). Cypermethrin, a synthetic pyrethroid, affects voltage-gated sodium channels, prolonging neuronal excitation and resulting in paralysis and death of insects (Gupta et al., 2021).

The pervasive application of these pesticides has led to environmental contamination, with residues detected in soil, water, and food products. Consequently, there is an increased risk of exposure to non-target species, including mammals. Studies have demonstrated that exposure to these pesticides can induce oxidative stress, hematological alterations, and histopathological changes in various organs (Bouabdallah et al., 2022; Hart & Ibeachu, 2022). For instance, dichlorvos exposure has been associated with hematotoxic and hepatotoxic effects in rats, characterized by alterations in red blood cell counts and liver enzyme activities (Celik et al., 2009). Similarly, cypermethrin exposure has been linked to

neurodegenerative changes in the striatum of adult Wistar rats, indicating its potential to induce oxidative stress and neuronal damage (Udodi et al., 2023).

Reproductive status, particularly the postpartum state, may influence an organism's susceptibility to toxicants. The postpartum period involves significant physiological changes, including hormonal fluctuations and alterations in metabolic and immune functions, which could modulate responses to environmental stressors. However, limited research has focused on comparing the effects of pesticide exposure between postpartum and non-postpartum females. Understanding these differences is crucial, as it may inform risk assessment and the development of protective measures for vulnerable populations.

This study aims to investigate the hematological and histological effects of combined exposure to dichlorvos, dimethoate, and cypermethrin in postpartum and non-postpartum female Wistar rats. By assessing parameters such as red and white blood cell counts, hemoglobin levels, and histopathological changes in reproductive organs, this research seeks to elucidate the potential differential impacts of pesticide mixtures based on reproductive status. The findings may contribute to a better understanding of the risks associated with pesticide exposure and the importance of considering physiological states in toxicological evaluations.

MATERIALS AND METHODS

Reagents and solvents were of analytical grade and are products of British Drug House, Poole, England.

This study was conducted to evaluate the biochemical and histopathological effects of a mixture of dichlorvos, dimethoate, and cypermethrin on female rats at various biological stages, including exposure, mating, pregnancy, and lactation.

A total of 64 female rats and 16 male rats of uniform strain, weight, and age were acquired for the study. The animals were acclimatized for a week before the commencement of the experiment to ensure their well-being and to minimize stress-related variability.

The female rats were divided into eight groups (A–H), with each group consisting of eight rats. The groups were exposed to varying doses of the chemical mixture, administered via a pre-determined and controlled route to ensure consistency in delivery. The exposure lasted for 28 days, during which the health and behavior of the rats were closely monitored. At the end of this period, four rats from each group (n=4) were randomly selected and sacrificed for haematological and histopathological analyses. These analyses provided baseline data on the effects of the chemical mixture during the exposure phase.

Following the sacrifice of the initial subset of rats, the remaining four rats in each group were exposed to two male rats per group to facilitate mating. Behavioral observations confirmed successful copulation, after which the male rats were removed to prevent additional stress and ensure the well-being of the females. The copulated female rats were monitored throughout their pregnancy for any health or behavioral changes. After delivery, the lactating rats were allowed to nurse their litters for 10 days. During this period, maternal care behaviors were observed, and the health and growth of the pups were recorded to assess potential transgenerational effects of the chemical exposure.

At the end of the 10-day lactation period, the lactating rats were sacrificed, and comprehensive haematological and histopathological analyses were performed. The data collected during both the exposure and lactation phases were analyzed using appropriate statistical tools to identify significant trends, dose-dependent effects, and potential long-term impacts of the chemical mixture.

Animals

Adult virgin female albino Wistar rats, aged 2–3 months and weighing 190–200 g, were used for this study. The animals were obtained from the Animal House of the Federal University of Petroleum Resources, Effurun. Upon acquisition, they were housed in cages, with five rats per cage, under controlled and hygienic conditions to ensure their health and well-being. The environmental conditions were maintained at a room temperature of 25 ± 2°C, relative humidity of 50 ± 10%, and a photoperiod of 12 hours of light and 12 hours of darkness.

The rats were provided with standard laboratory pelleted rodent feed and clean drinking water *ad libitum* throughout the experimental period. The cages and bedding materials were regularly cleaned and replaced to maintain a high standard of hygiene. This setup ensured that the animals were in optimal health, minimizing external stressors and allowing for reliable and consistent experimental results. All experimental procedures were carried out in accordance with ethical guidelines for the care and use of laboratory animals.

Dose Levels

Dichlorvos, dimethoate, and cypermethrin, all obtained from Hubei Sanonda Co. Ltd, China, were used in this study. These agrochemicals were purchased from a licensed agrochemical shop and diluted with clean water as per domestic usage guidelines. The dose combinations were prepared in specific ratios for each experimental group. For group B, C, and D, the chemicals were used individually at a 1:1 dilution. For groups E, F, and G, a combination of two chemicals was prepared in a 1:0.5:0.5 ratio. For group H, a mixture of all three chemicals was prepared in a 1:0.33:0.33:0.33 ratio. These freshly prepared solutions were used daily for a continuous exposure period of 28 days.

The solutions were sprayed into a poorly ventilated compartment where the animal cages were kept, simulating conditions of domestic pesticide use. A control group (Group A) was maintained, exposed only to water sprayed in the same manner. The exposure was designed to replicate real-

life scenarios where animals might come into contact with pesticide residues in a confined space.

The animals in all groups were monitored daily, and humane care was ensured throughout the study, following the guidelines outlined in the *Guide for the Care and Use of Laboratory Animals* by the National Academy of Sciences and published by the National Institute of Health. This ensured adherence to ethical standards for the welfare of laboratory animals while providing reliable data on the biochemical and toxicological impacts of the chemical exposure.

The treatment groups were as follows:

- **Group A (Control):** Exposed to sprayed water.
- **Group B:** Exposed to dichlorvos.
- **Group C:** Exposed to dimethoate.
- **Group D:** Exposed to cypermethrin.
- **Group E:** Exposed to a mixture of dichlorvos and dimethoate.
- **Group F:** Exposed to a mixture of dichlorvos and cypermethrin.
- **Group G:** Exposed to a mixture of dimethoate and cypermethrin.
- **Group H:** Exposed to a mixture of dichlorvos, dimethoate, and cypermethrin.

Mating and Fertility Assessment

On post-treatment day (PTD) 29, the remaining treated female rats (n = 4 per group) were cohabited with proven fertile adult male rats in a 2:1 ratio to assess their mating and fertility status. Daily vaginal smears were collected from the cohabited females, and the presence of sperm in the vaginal smear was used as confirmation of copulation. The day on which sperm-positive vaginal smears were observed was recorded as gestational day zero (GD 0). The time taken for each female to exhibit sperm-positive smears was carefully recorded to evaluate potential effects of the treatments on mating efficiency and fertility.

Blood Sampling

Following 28 days of treatment, blood samples were collected from the treated female rats under light anesthesia using chloroform. Blood was obtained from the dorsal aorta of four females per group and divided into heparinized tubes. The blood in heparinized tubes was used for hematological analysis. Portions of tissues (ovary and uterus) obtained from the experimental rats were fixed in 10% buffered neutral formaline (BNF) for histopathological analysis.

Haemoglobin concentration of the blood of experimental animals was determined following the method described by Mitruka and Rawnsley (1977). Histological study on tissues (Ovary and uterus) obtained from experimental rats was carried out following the method described by Drury and Wallington (1973).

Statistical Analyses

All numerical results were obtained from the eight (8) groups (control and treated). Data were presented as mean±SEM and analysed using one way analysis of variance (ANOVA) and Duncan Multiple Range Test using SPSS-30.0 (Statistical packages for social Scientists – version 30.0) statistical program. P values<0.05 were considered significant.

RESULTS

This comparative summary examines the haematological properties of both female Wistar albino rats and postpartum Wistar albino rats exposed to mixtures of Dichlorvos, Dimethoate, and Cypermethrin, as presented in Tables 1 and 2.

In female rats, RBC counts show a significant decrease in Group B (Dichlorvos) and Group G (Dimethoate + Cypermethrin). Similarly, postpartum rats experience a decrease in RBC in Group B (Dichlorvos), although postpartum rats maintain relatively higher RBC counts in Group E (Dichlorvos + Dimethoate) and Group F (Dichlorvos + Cypermethrin) compared to non-postpartum female rats. Female rats show the most notable reduction in HB levels in Group B (Dichlorvos) and Group F (Dichlorvos + Cypermethrin). In postpartum rats, HB reduction is also observed in Group B (Dichlorvos), but postpartum rats maintain slightly higher HB levels overall compared to non-postpartum females. In female rats, platelet counts increase significantly in groups exposed to Dimethoate and Cypermethrin, particularly in Group F (Dichlorvos + Cypermethrin). Postpartum rats show a similar trend, with Group F displaying the highest platelet levels. Generally, postpartum rats maintain higher platelet counts across all groups compared to female rats. Among female rats, the lowest MCV values are observed in Group B (Dichlorvos). Postpartum rats also show lower MCV in Group B, though they tend to maintain slightly higher MCV values across all groups compared to non-postpartum females. Female rats experience significant reductions in MCH in Group B (Dichlorvos). A similar trend is observed in postpartum rats, although postpartum rats maintain higher MCH values overall. Notably, Groups F and G show a reduction in MCH among postpartum rats. In female rats, Group B (Dichlorvos) exhibits the lowest MCHC, indicating a strong impact of Dichlorvos on hemoglobin concentration. Postpartum rats also show a reduction in MCHC in Group B, though they retain slightly higher values than non-postpartum females, suggesting a modest resilience. For female rats, PCV is significantly elevated in Group F (Dichlorvos + Cypermethrin) and Group G (Dimethoate + Cypermethrin). This trend is consistent in postpartum rats, who generally have higher PCV values across all groups, especially in Groups F and G.

Both female and postpartum rats show elevated WBC across exposed groups, with Group G (Dimethoate + Cypermethrin)

exhibiting the highest counts. Postpartum rats tend to have generally higher WBC counts across groups compared to non-postpartum females, suggesting a robust immune response. Both sets of rats show increases in neutrophils and eosinophils across exposed groups. Lymphocyte counts are particularly higher in postpartum rats, especially in Groups G and H, indicating an active immune response triggered by chemical exposure. An increase in monocytes is observed across chemically exposed groups in both sets of rats, with Groups F and G showing the most pronounced increases in monocyte counts for both female and postpartum rats.

In conclusion, both female and postpartum Wistar albino rats experience substantial haematological changes due to pesticide exposure, with Dichlorvos having the most significant toxic effects. Postpartum rats generally retain higher values across most haematological parameters, suggesting a degree of physiological resilience, likely associated with postpartum physiological adaptations. However, the toxicity trends remain consistent across both groups, with Group B (Dichlorvos) and Dichlorvos-containing combinations showing the most detrimental effects on haematological health.

Table 1: HAEMATOLOGY PROPERTIES OF FEMALE WISTAR ALBINO RATS EXPOSED TO MIXTURE OF DICHLORVOS, DIMETHOATE AND CYPERMETHRIN.

	A	B	C	D	E	F	G	H
RBC MEAN	8.97±0.645 a	7.25±0.190 b	8.34±0.645 a	8.82±0.645 a	8.57±0.645 a	8.01±0.002 a	7.58±0.645 b	7.61±0.003 b
HB (g/dl)	14.01±0.120a	11.31±0.300b	13.00±0.110c	13.76±0.090c	13.37±0.226c	12.50±0.005d	11.82±0.049b	11.87±0.004b
PLATELETS (x103/mm³)	252.09±4.809a	265.19±6.985b	283.33±4.170c	257.13±3.140a	264.71±3.353b	293.16±4.093d	277.31±4.077e	278.50±4.090e
MCV (μ³)	55.00±0.474a	44.40±1.174b	51.07±1.344a	54.02±0.906a	52.50±1.759a	49.07±0.017c	46.42±1.798bc	46.62±0.015b
MCH (μμg)	16.05±0.137a	12.96±0.342b	14.90±0.665c	15.76±0.557d	15.32±1.391d	14.27±0.052c	13.55±0.301e	13.60±0.005e
MCHC (%)	31.08±0.269a	25.08±0.660b	28.86±0.376c	30.52±0.314d	29.66±0.405d	27.73±0.009e	26.23±0.088e	26.34±0.009e
PCV (%)	47.05±0.301a	61.02±1.607b	65.17±1.243b	51.45±0.981c	57.90±0.787c	67.46±0.021b	63.81±0.170b	64.09±0.019b
WBC (x103/mm³)	9.95±0.028 a	10.64±0.049b	10.48±0.028b	10.13±0.028b	10.30±1.104b	10.45±0.003b	10.80±0.413b	10.53±0.003b
NEUTROPHILS (%)	6.43±0.018 a	6.89±0.032 a	6.79±0.019 a	6.55±0.019 a	6.67±0.030 a	6.76±0.002 a	6.99±0.201 a	6.82±0.003 a
EOSINPHILS (%)	0.37±0.004 a	0.43±0.003 b	0.42±0.004 b	0.39±0.003 ab	0.41±0.019 b	0.43±0.000 b	0.44±0.129 b	0.43±0.000 b
BASOPHILS (%)	0.01±0.003 a	0.04±0.000 b	0.04±0.003 b	0.02±0.003 ab	0.03±0.003 b	0.04±0.000 b	0.04±0.008 b	0.04±0.000 b
LYMPHOCYTES (%)	61.56±0.161a	65.56±0.297b	64.61±0.168b	62.56±0.163a	63.58±0.003ab	64.38±0.016b	66.55±0.000b	64.90±0.017b
MONOCYTES (%)	0.26±0.003 a	0.31±0.003 b	0.30±0.003 b	0.27±0.003 a	0.29±0.165 b	0.31±0.000 b	0.32±1.237 b	0.31±0.000 b

Calculated values are means of four determinations ± SEM. Values in the same row bearing different alphabets are significantly different (p<0.05).

Table 2: HAEMATOLOGY PROPERTIES OF POSTPARTUM FEMALE WISTAR ALBINO RATS EXPOSED TO MIXTURE OF DICHLORVOS, DIMETHOATE AND CYPERMETHRIN.

PARAMETERS	A	B	C	D	E	F	G	H
RBC (X106/mm3)	9.03±0.062a	7.65±0.136b	8.53±0.116c	8.95±0.099c	8.65±0.240c	8.21±0.003c	7.81±0.052b	7.85±0.003b
HB (g/dl)	15.85±0.113a	13.34±0.247b	14.93±0.210bc	15.70±0.180c	15.16±0.436c	14.35±0.005bc	13.62±0.095b	13.69±0.005b
PLATELETS (x103/mm3)	276.47±6.272a	298.08±6.073b	310.72±6.977b	281.99±6.398b	292.18±5.026b	322.94±0.123c	305.03±2.343b	306.82±0.117b
MCV (µ3)	58.41±0.466a	48.08±1.017b	54.64±0.865c	57.79±0.739bc	55.57±1.795bc	52.24±0.021b	49.25±0.392b	49.55±0.020b
MCH (µµg)	16.43±0.185a	12.32±0.405b	14.93±0.344bc	16.19±0.294c	15.30±0.714c	13.98±0.008b	12.79±0.156b	12.91±0.008b
MCHC (%)	36.26±0.311a	29.36±0.679b	33.74±0.578b	35.85±0.494b	34.37±1.199b	32.14±0.014b	30.14±0.262b	30.34±0.013b
PCV (%)	49.41±0.365a	64.99±1.296b	67.65±1.504b	53.72±1.187c	59.68±0.860c	70.30±0.026d	66.48±0.500b	66.86±0.025b
WBC (x103/mm3)	10.70±0.059a	11.88±0.067b	11.65±0.062b	11.01±0.060b	11.30±0.040b	11.60±0.006b	12.40±0.395c	11.75±0.006b
NEUTROPHILS(%)	6.78±0.020a	7.18±0.022a	7.10±0.021a	6.89±0.020a	6.98±0.013a	7.09±0.002a	7.34±0.128a	7.13±0.002a
EOSINOPHILS (%)	0.42±0.004a	0.50±0.002b	0.48±0.004b	0.44±0.004a	0.46±0.003ab	0.49±0.000b	0.51±0.010b	0.49±0.000b
BASOPHILS (%)	0.03±0.011a	0.05±0.000b	0.05±0.009b	0.02±0.005a	0.04±0.002b	0.05±0.001b	0.05±0.000b	0.04±0.012b
LYMPHOCYTES (%)	66.69±0.589a	78.52±0.706b	76.16±0.618b	69.80±0.599a	72.69±0.397b	75.58±0.060b	84.05±4.189c	77.17±0.061b
MONOCYTES (%)	0.21±0.003a	0.27±0.001b	0.26±0.003b	0.23±0.003a	0.24±0.002ab	0.27±0.000b	0.28±0.007b	0.27±0.000b

Calculated values are means of four determinations ± SEM. Values in the same row bearing different alphabets are significantly different ($p<0.05$).

The histopathology micrographs provided in Plates 1 to 8 reveal various structural changes in the uterine tissue of non-postpartum female Wistar albino rats exposed to different pesticides.

Plate 1 (Group A): The uterus of rats exposed only to sprayed water serves as the control, showing a normal histological structure. The endometrial lining (EL) appears intact and is underlaid by a stroma (ST) that contains well-organized endometrial glands (EG). This image represents the standard, healthy uterine morphology, which is crucial for comparing the structural integrity observed in other groups.

Plate 2 (Group B): In the uterus of rats exposed to dichlorvos, structural modifications are evident. The endometrial lining (EL) remains identifiable, but the underlying stroma has developed fibrous characteristics (FS). Notably, the endometrial gland (EG) appears dilated and contains secreting epithelium, indicating a response likely due to dichlorvos exposure. These changes may suggest an adaptive response or initial damage due to dichlorvos.

Plate 3 (Group C): The uterine tissue of rats exposed to dimethoate shows a distinct mucosal membrane (MM) supported by a fibrocollagenous subepithelium (SE). Numerous vascular spaces (VS) are present, indicating possible vascularization changes in response to dimethoate. These features might point to altered vascular integrity, potentially due to inflammatory or reactive processes.

Plate 4 (Group D): The uterus of rats exposed to cypermethrin reveals an ulcerated mucosal membrane (MM), and the subepithelium (SE) displays vascularization (VS). Ulceration suggests a more severe form of tissue damage or necrosis, which cypermethrin may have induced. This damage could indicate a breakdown in the structural integrity of the mucosal membrane.

Plate 5 (Group E): The combined exposure to dichlorvos and dimethoate in this group results in notable focal mucosal ulceration (FU). Additionally, inflammatory cells infiltrate the fibrocollagenous stroma (FS), which implies an inflammatory response. The presence of inflammatory cells highlights the tissue's reaction to the combined pesticide exposure, suggesting heightened immune activity as the tissue attempts to counteract damage.

Plate 6 (Group F): In the uterus of rats exposed to dichlorvos and cypermethrin, the mucosal membrane (MM) appears normal, and the subepithelium comprises fibrocollagenous connective tissue (SE) with abundant vascular spaces (VS). This image shows less apparent damage compared to some other groups, implying a potentially reduced or balanced response to this combination of pesticides.

Plate 7 (Group G): Exposure to dimethoate and cypermethrin results in a normal-looking endometrial membrane (EM), with the subepithelium containing numerous small glands (EG) supported by fibromyxoid stroma (ST). This indicates that this particular combination might have less toxic impact on the endometrial architecture than other combinations.

Plate 8 (Group H): The uterus of rats exposed to the combination of dichlorvos, dimethoate, and cypermethrin shows an endometrial membrane with patchy ulceration areas (MU). The underlying fibromyxoid stroma (ST) supports small glands (EG). The ulcerations observed suggest considerable tissue damage, possibly due to cumulative or synergistic toxic effects of the three pesticides combined.

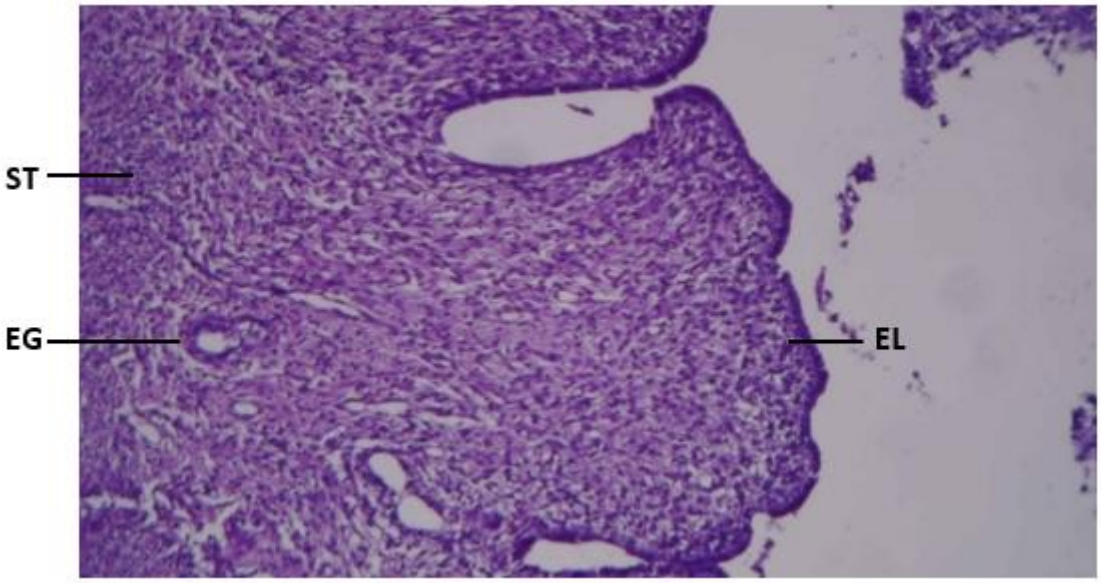

Plate 1. Group A: Histopathology micrograph of uterus of non-postpartum female wistar albino rats exposed to sprayed water showing normal endometrial lining (EL), below which is the stroma (ST), with embedded endometrial glands (EG): H&E 100 X

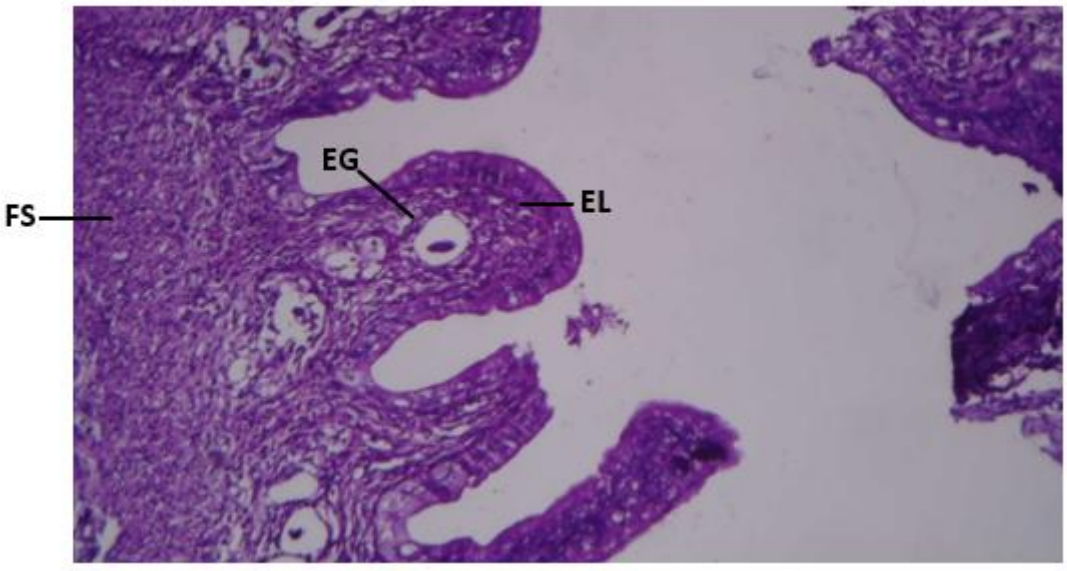

Plate 2. Group B: Histopathology micrograph of uterus of non-postpartum female wistar albino rats exposed to dichlorvos showing: endometrial lining (EL), below which is a fibrous stroma (FS), supporting dilated gland (EG) containing secreting epithelium: H&E 100 X

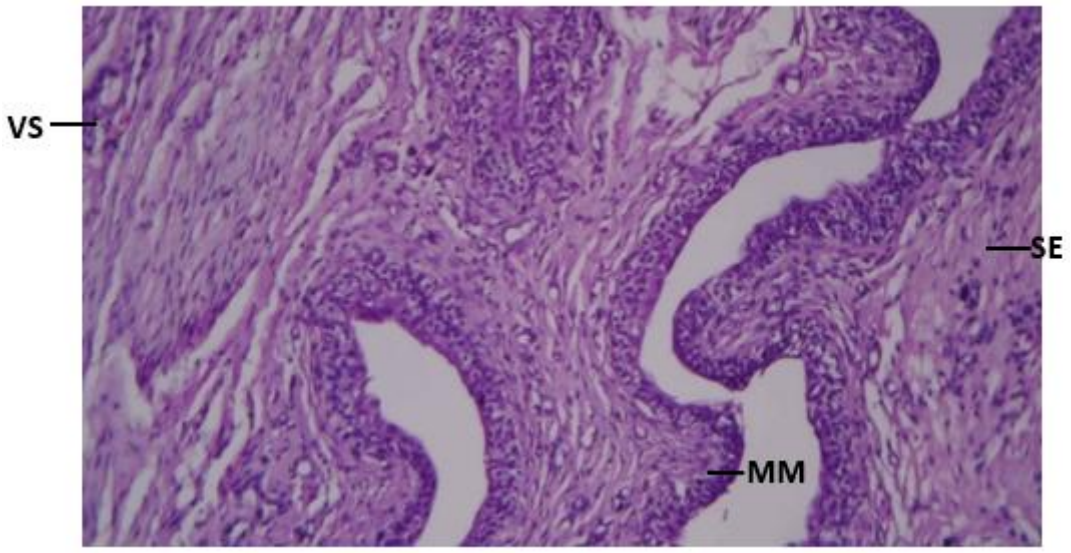

Plate 3. Group C: Histopathology micrograph of uterus of non-postpartum female wistar albino rats exposed to dimethoate showing: mucosal membrane (MM), below which is a fibrocollagenoussubepitheluim (SE), supported by numerous vascular spaces (VS): H&E 100 X

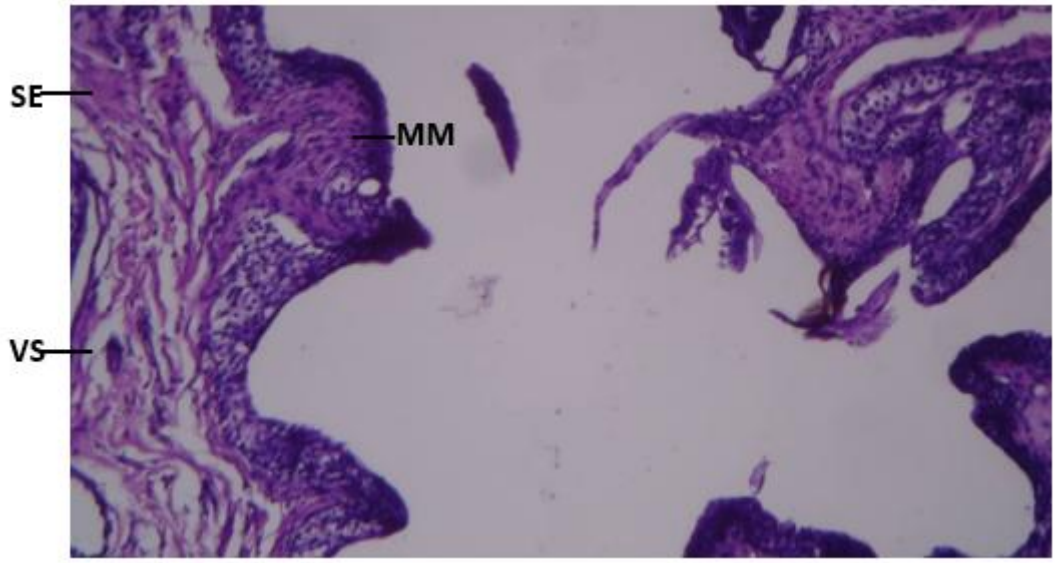

Plate 4. Group D: Histopathology micrograph of uterus of non-postpartum female wistar albino rats exposed to cypermethrin showing: ulcerated mucosal membrane (MM): the fibrocollagenoussubepitheluim (SE) is vascularized (VS): H&E 100 X

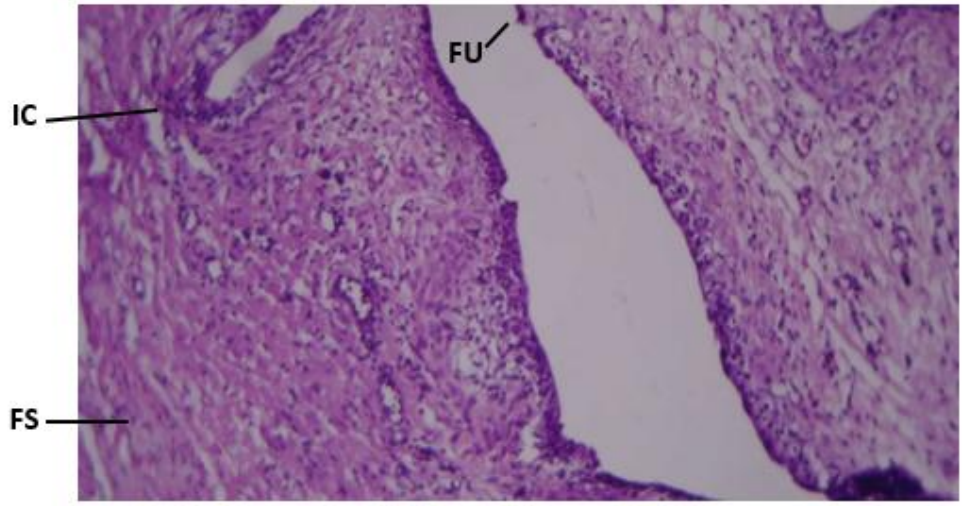

Plate 5. Group E: Histopathology micrograph of uterus of non-postpartum female wistar albino rats exposed to dichlorvos and dimethoate showing: focal mucosal ulceration (FU): There are infiltrates of inflammatory cells (IC), in the fibrocollagenous stroma (FS): H&E 100 X

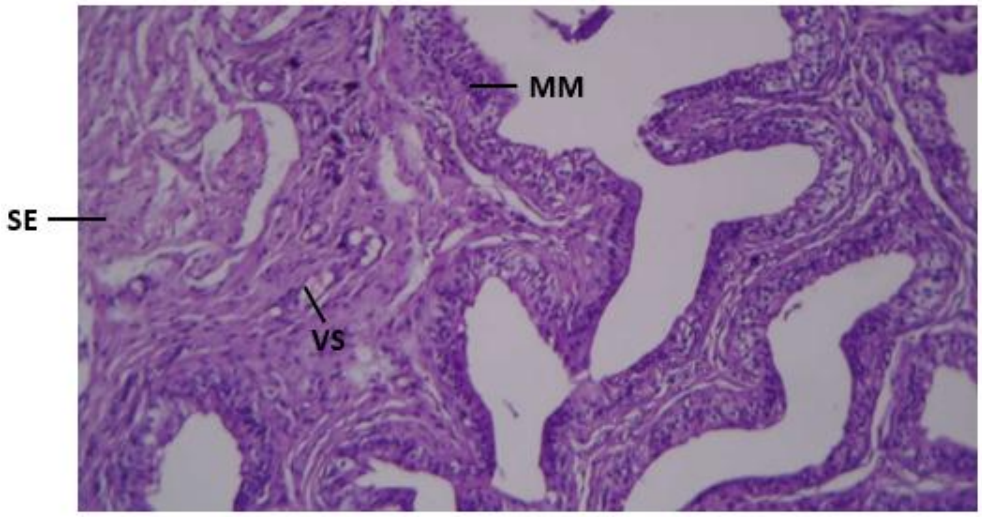

Plate 6. Group F: Histopathology micrograph of uterus of non-postpartum female wistar albino rats exposed to dichlorvos and cypermethrin showing normal mucosal membrane (MM). The subepithelium is composed of fibrocollagenous connective tissue (SE) with numerous vascular spaces (VS): H&E 100 X

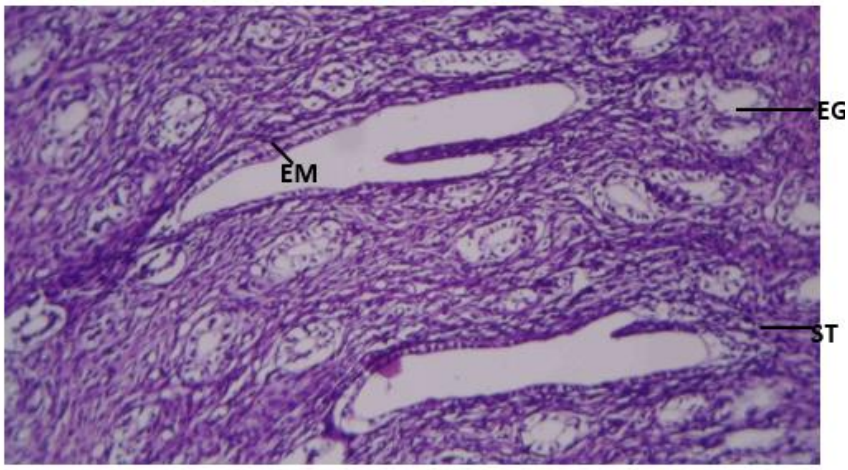

Plate 7. Group G: Histopathology micrograph of uterus of non-postpartum female wistar albino rats exposed to dimethoate and cypermethrin showing normal endometrial membrane (EM): The subepithelium is composed of numerous small glands (EG) supported by a fibromyxoidstroma (ST): H&E 100 X

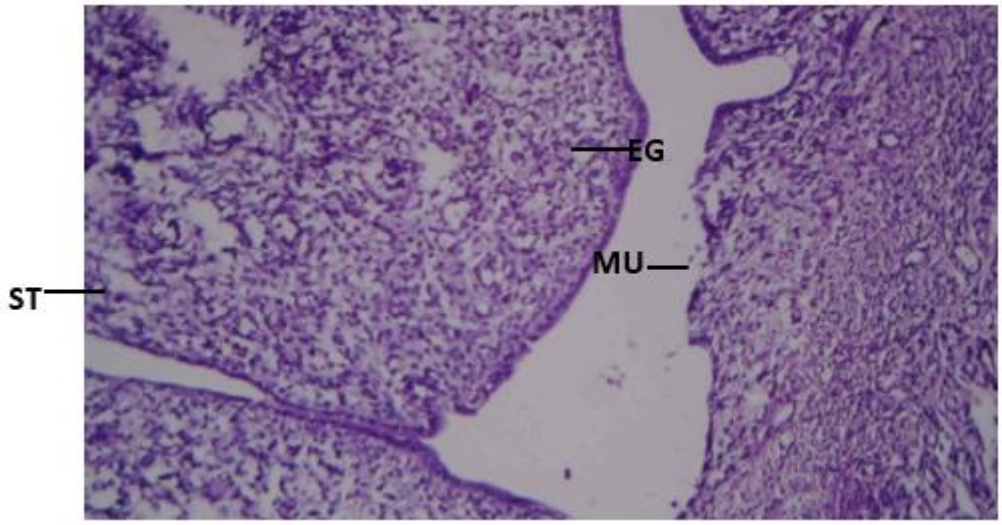

Plate 8. Group H: Histopathology micrograph of uterus of non-postpartum female wistar albino rats exposed to dichlorvos, dimethoate, and cypermethrin showing endometrial membrane with patchy areas of ulceration (MU): The subepithelium is composed of small glands (EG) supported by a fibromyxoidstroma (ST): H&E 100 X

The histopathology micrographs provided (Plates 9 to 16) depict the ovarian tissue of non-postpartum female Wistar albino rats exposed to various pesticides. The structural alterations observed vary depending on the specific pesticide or combination of pesticides applied.

Plate 9 (Group A): This control image represents the ovary of rats exposed only to sprayed water, showing a normal histological structure. The coelomic epithelium (CE) is intact, the stromal tissue (ST) is well-organized, and there is a clear presence of corpus luteum (CL) and developing follicles (DF). This normal architecture serves as a baseline for assessing deviations in ovarian structure in other groups.

Plate 10 (Group B): The ovarian tissue of rats exposed to dichlorvos exhibits noticeable pathological changes. There is significant follicular degeneration (FD), accompanied by a heavy infiltration of inflammatory cells (IC) in the stroma. The stromal tissue also shows signs of severe congestion (SC) and myxoid degeneration (SD). These findings indicate a strong inflammatory response and compromised structural integrity, likely as a direct result of dichlorvos exposure.

Plate 11 (Group C): In the ovaries of rats exposed to dimethoate, similar adverse changes are observed. Follicular degeneration (FD) is present along with stromal myxoid degeneration (MD) and inflammatory cell infiltrates (IC). The presence of these degenerative changes suggests a toxic effect of dimethoate on the ovarian tissue, leading to structural breakdown and inflammatory responses.

Plate 12 (Group D): The exposure to cypermethrin results in severe degenerative changes in the ovarian tissue. There is marked follicular degeneration (FD), coupled with severe stromal congestion (SC) and myxoid stromal degeneration (SD). Additionally, there is a notable infiltration of inflammatory cells (IC). The extent of degeneration and congestion in this group indicates a potent disruptive impact of cypermethrin on ovarian morphology.

Plate 13 (Group E): The ovarian tissue of rats exposed to a combination of dichlorvos and dimethoate shows follicular degeneration (FD) and myxoid stromal degeneration (MD), along with stromal congestion (SC). Although the damage is significant, the absence of inflammatory cell infiltrates suggests a slightly reduced inflammatory response compared to some other combinations, although structural integrity remains compromised.

Plate 14 (Group F): In rats exposed to dichlorvos and cypermethrin, severe ovarian degeneration is evident. There is marked follicular degeneration (FD), accompanied by myxoid stromal degeneration (MD), stromal congestion (SC), and a notable infiltration of inflammatory cells (IC). The severity of these degenerative changes suggests a potentially synergistic effect of dichlorvos and cypermethrin, leading to both inflammatory and structural deterioration in the ovarian tissue.

Plate 15 (Group G): Exposure to a combination of dimethoate and cypermethrin similarly results in severe follicular degeneration (FD) and stromal congestion (SC), with inflammatory cell infiltration (IC) present. The combination of these pesticides appears to exacerbate the degenerative effects, suggesting a heightened toxic impact on the ovarian tissue as compared to individual exposures.

Plate 16 (Group H): The combined exposure to dichlorvos, dimethoate, and cypermethrin leads to extensive damage in the ovarian tissue. There is severe follicular degeneration (FD), stromal congestion (SC), and a pronounced infiltration of inflammatory cells (IC). This triad of severe degenerative, congestive, and inflammatory changes illustrates the cumulative toxic impact of simultaneous exposure to these three pesticides, resulting in substantial structural and inflammatory damage

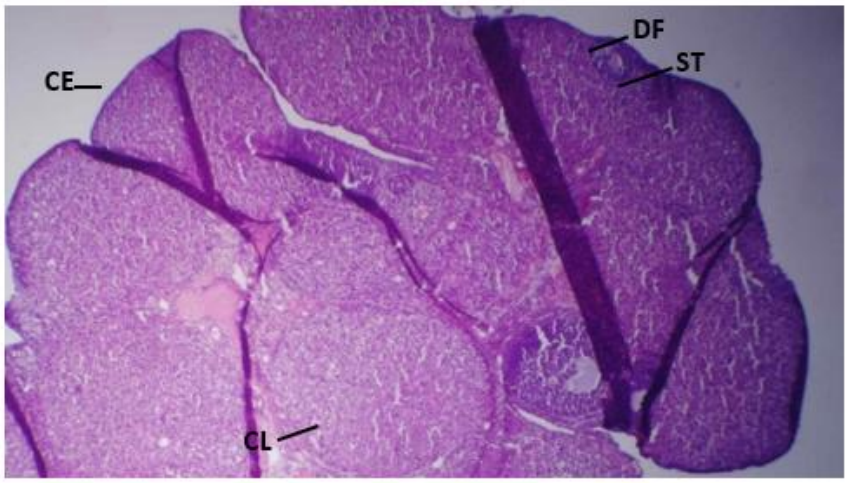

Plate 9. Group A: Histopathology micrograph of ovary of non-postpartum female wistar albino rats exposed to sprayed water showing normal architecture coelomic epithelium (CE), stromal (ST), corpus luteum (CL) and developing follicles (DF): H & E 40 X

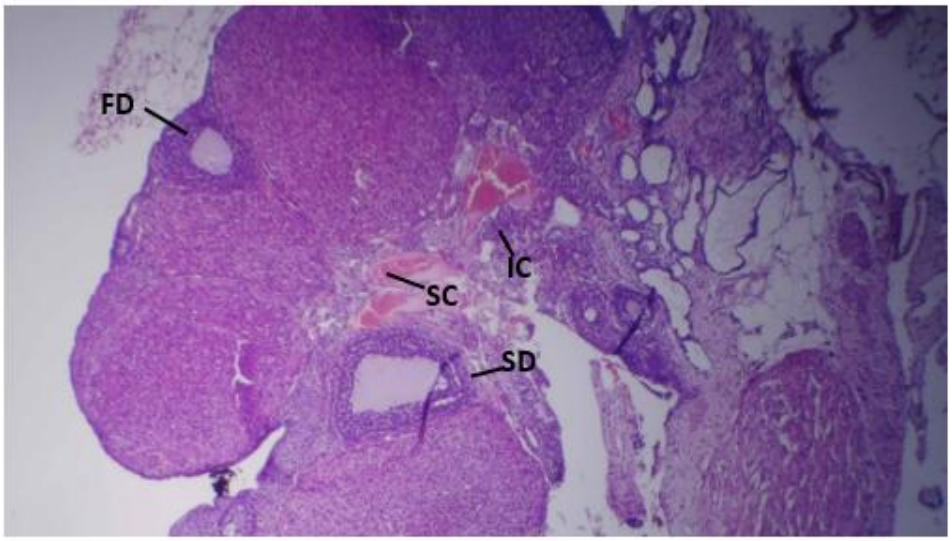

Plate 10. Group B: Histopathology micrograph of ovary of non-postpartum female wistar albino rats exposed to dichlorvos showing: follicular degeneration (FD), heavy stromal infiltrates of inflammatory cells (IC), severe stromal congestion (SC) and stromal myxoid degeneration (SD): H&E 40 X

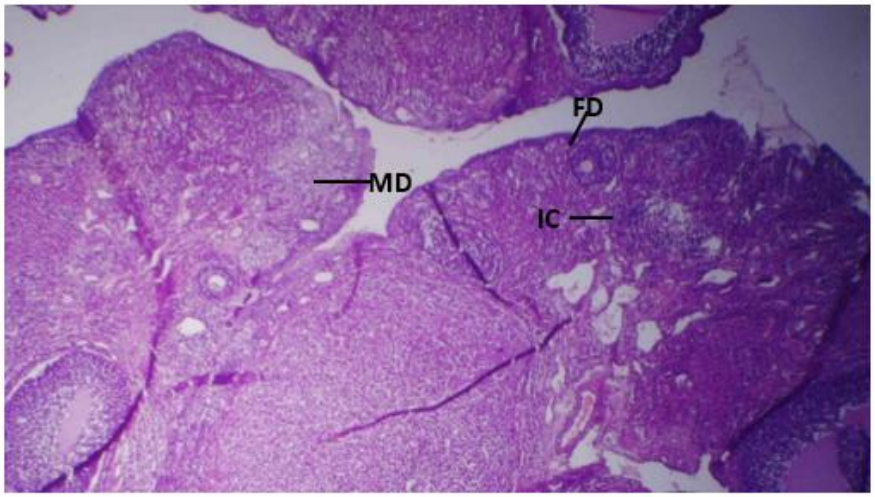

Plate 11. Group C: Histopathology micrograph of ovary of non-postpartum female wistar albino rats exposed to dimethoate showing: follicular degeneration (FD), myxoid stromal degeneration (MD) and infiltrates of inflammatory cells (IC): H&E 40 X

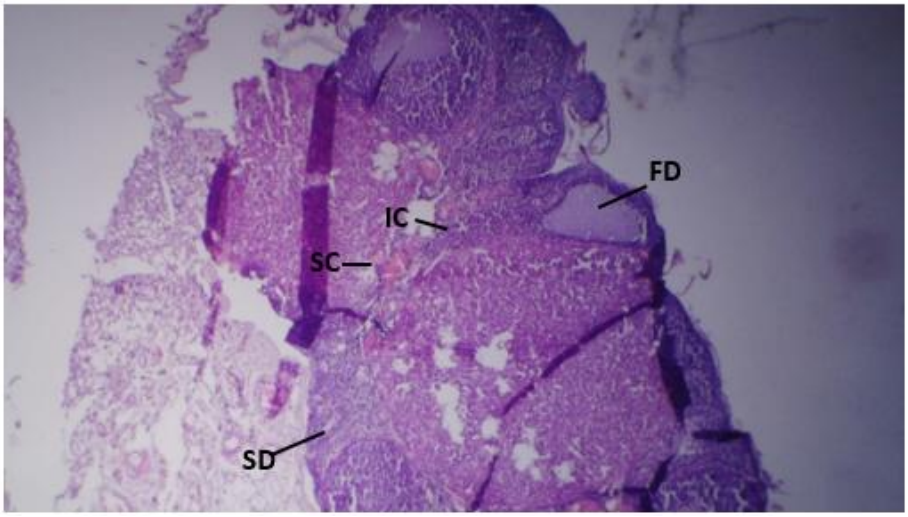

Plate 12. Group D: Histopathology micrograph of ovary of non-postpartum female wistar albino rats exposed to cypermethrin showing: severe follicular degeneration (FD), severe stromal congestion (SC), severe myxoid stromal degeneration (SD) and infiltrates of inflammatory cells (IC): H&E 40 X

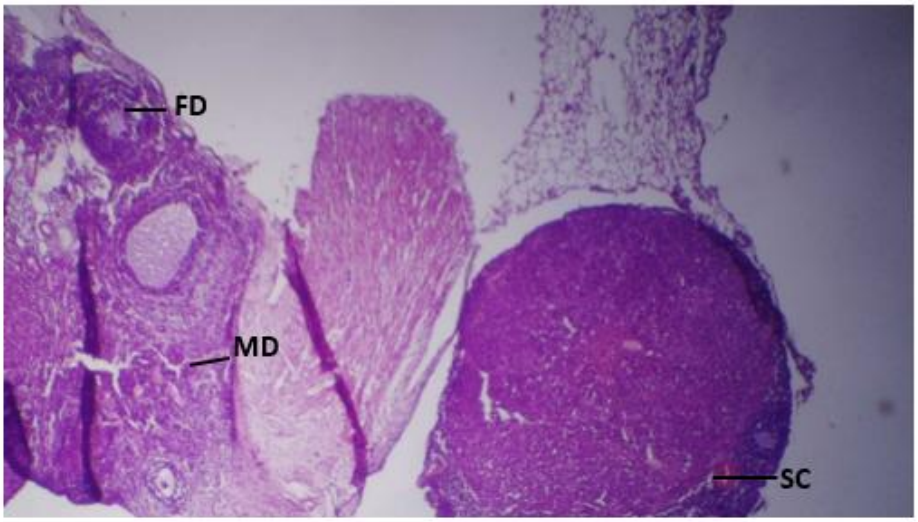

Plate 13. Group E: Histopathology micrograph of ovary of non-postpartum female wistar albino rats exposed to dichlorvos and dimethoate showing: follicular degeneration (FD), myxoid stromal degeneration (MD) and stromal congestion (SC): H&E 40 X

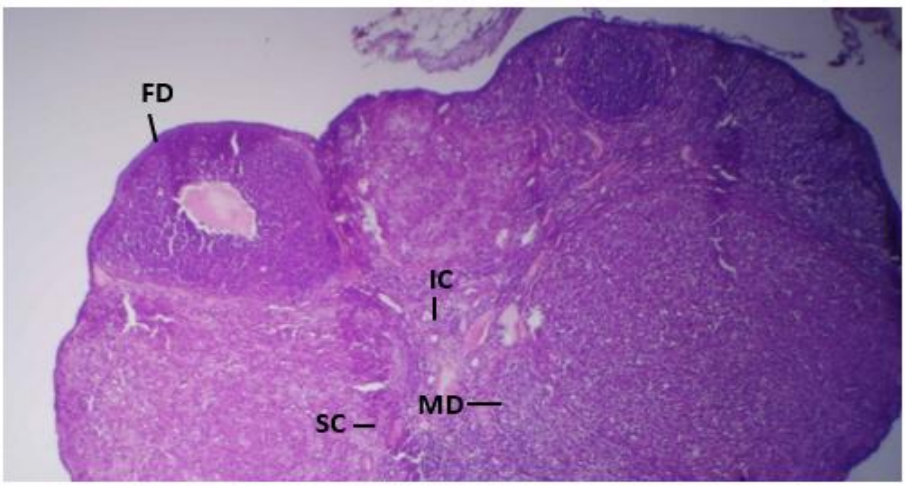

Plate 14. Group F: Histopathology micrograph of ovary of non-postpartum female wistar albino rats exposed to dichlorvos and cypermethrin showing severe follicular degeneration (FD), stromal myxoid degeneration (MD), stromal congestion (SC) and stromal infiltrates of inflammatory cells (IC): H&E 40 X

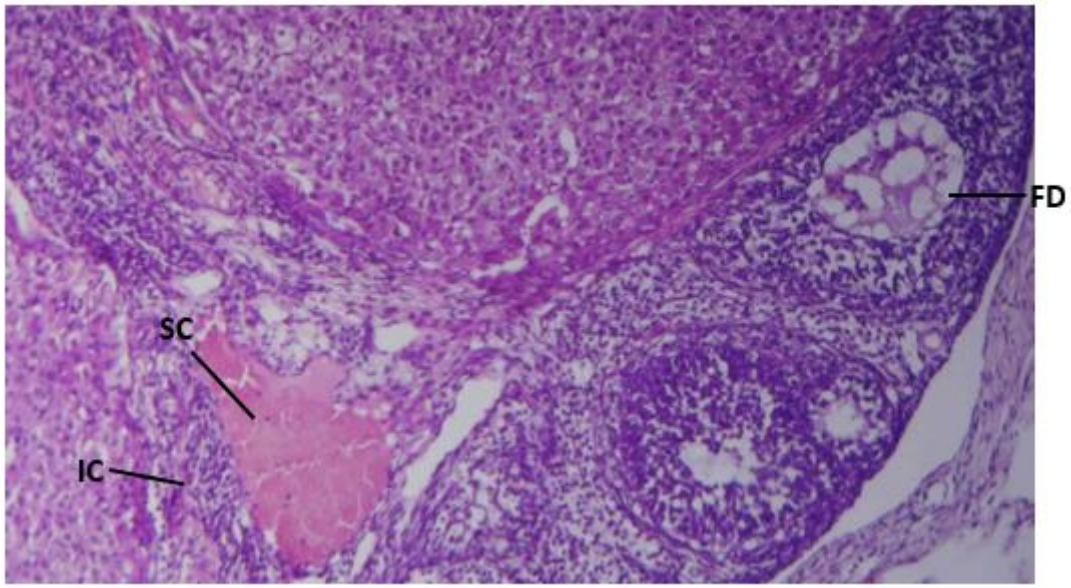

Plate 15. Group G: Histopathology micrograph of ovary of non-postpartum female wistar albino rats exposed to dimethoate and cypermethrin showing severe follicular degeneration (FD), stromal congestion (SC) and stromal infiltrates of inflammatory cells (IC): H&E 100 X

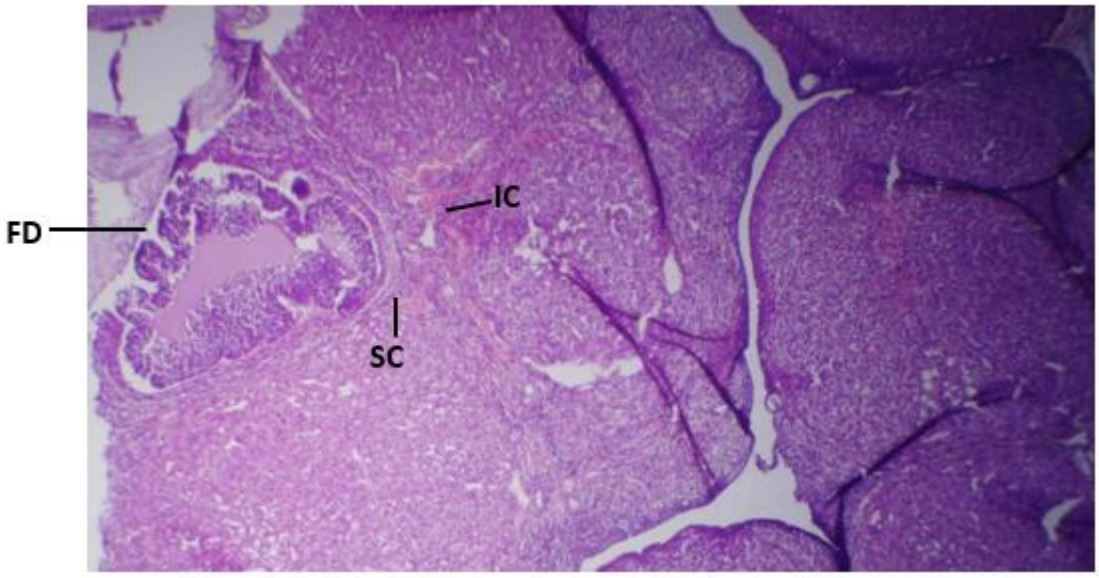

Plate 16. Group H: Histopathology micrograph of ovary of non-postpartum female wistar albino rats exposed to dichlorvos, dimethoate, and cypermethrin showing severe follicular degeneration (FD), severe stromal congestion (SC) and severe stromal infiltrates of inflammatory cells (IC): H&E 40 X

The histopathology micrographs in Plates 17 to 24 provide insight into the effects of pesticide exposure on the uterine tissue of postpartum female Wistar albino rats. The findings show a progression of damage based on the type and combination of pesticides used. Here is a detailed interpretation of each plate.

Plate 17 (Group A): This control image of the uterus in postpartum rats exposed to sprayed water reveals normal histological features. The uterine cavity (UC), endometrial lining (EL), endometrial glands (EG), and stroma (ST) all appear intact and well-organized. This baseline image serves as a reference to identify pathological deviations in the pesticide-exposed groups.

Plate 18 (Group B): The uterus of rats exposed to dichlorvos exhibits marked pathological changes. There is extensive ulceration of the endometrial lining (EU), coupled with stromal myxoid degeneration (MD) and a substantial infiltration of inflammatory cells (IC). These findings indicate a strong inflammatory response and structural degradation, likely due to dichlorvos toxicity, which compromises the endometrial integrity.

Plate 19 (Group C): In the uterus of rats exposed to dimethoate, similar histopathological features are observed,

including ulceration of the endometrial lining (EU), stromal myxoid degeneration (MD), and infiltration of inflammatory cells (IC). These alterations point to a toxic impact on uterine tissue, resulting in inflammation and degeneration of both the endometrial and stromal layers.

Plate 20 (Group D): Exposure to cypermethrin causes stromal myxoid degeneration (MD) and a prominent infiltration of inflammatory cells (IC) within the uterine tissue. The absence of ulceration in this group suggests a slightly reduced level of damage compared to dichlorvos and dimethoate; however, the degenerative changes still highlight a toxic response to cypermethrin.

Plate 21 (Group E): The combination of dichlorvos and dimethoate exposure in postpartum rats results in significant histological damage. There is evident ulceration in the endometrial lining (EU), along with epithelial vacuolation (EV) and vascular degeneration (VD) in the stroma. These features indicate structural breakdown and inflammation, suggesting that the combined exposure has an additive or synergistic effect, worsening the uterine tissue's integrity and vascular stability.

Plate 22 (Group F): The uterine tissue of rats exposed to a combination of dichlorvos and cypermethrin shows severe ulceration of the endometrial lining (EU), myxoid degeneration in the stroma (MD), and an influx of inflammatory cells (IC). The severity of the ulcerative damage and inflammatory infiltration indicates an intensified response due to the combined exposure to these pesticides.

Plate 23 (Group G): In rats exposed to dimethoate and cypermethrin, there is marked myxoid degeneration (MD) in the endometrial stroma, as well as severe degeneration of the endometrial glands (GD). These changes suggest that this pesticide combination disrupts glandular integrity and stroma structure, contributing to the overall compromised architecture of the uterine tissue.

Plate 24 (Group H): The combined exposure to dichlorvos, dimethoate, and cypermethrin results in severe vacuolation of the endometrial lining (EV), extensive stromal infiltration of inflammatory cells (IC), and pronounced myxoid degeneration (MD) within the stroma. This triad of vacuolation, degeneration, and inflammation reflects the cumulative toxic effect of all three pesticides, leading to significant structural and inflammatory damage within the uterus.

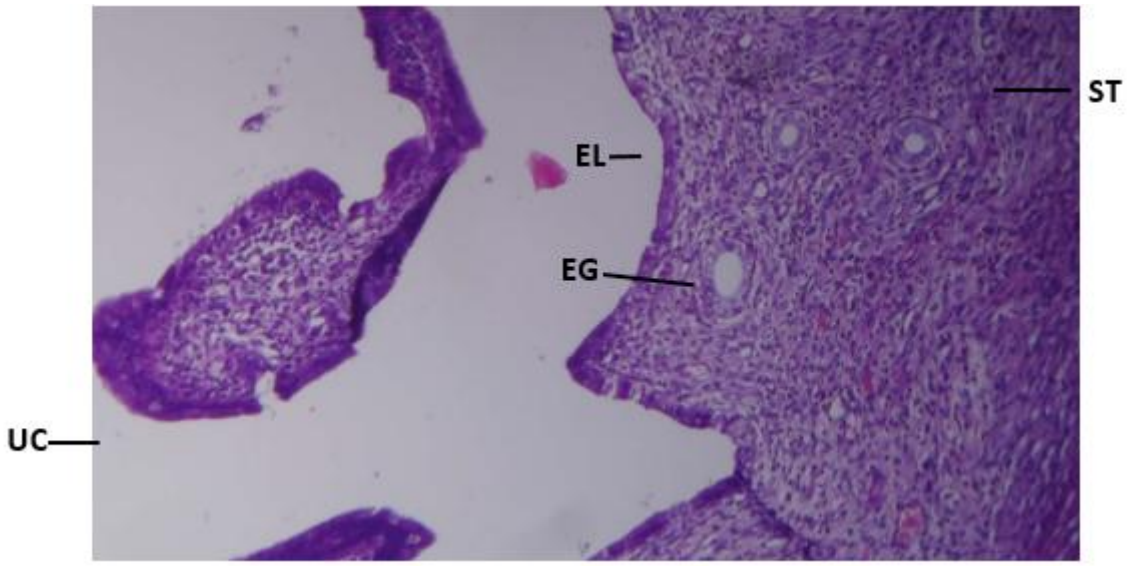

Plate 17. Group A: Histopathology micrograph of uterus of postpartum female wistar albino rats exposed to sprayed water showing normal architecture: uterine cavity (UC), endometrial lining (EL), endometrial glands (EG) and stroma (ST): H&E 100 X

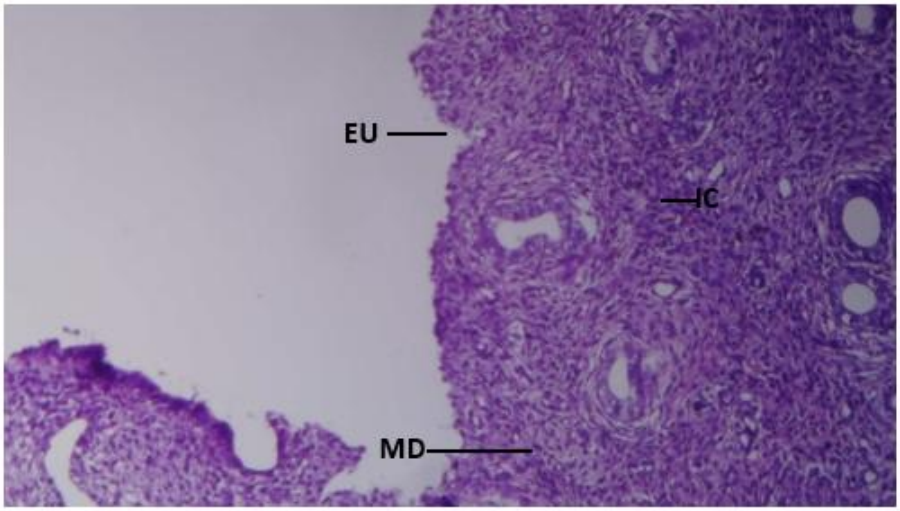

Plate 18. Group B: Histopathology micrograph of uterus of postpartum female wistar albino rats exposed to dichlorvos showing: extensive endometrial lining ulceration (EU), stromal myxoid degeneration (MD) and stromal infiltrates of inflammatory cells (IC): H&E 100 X

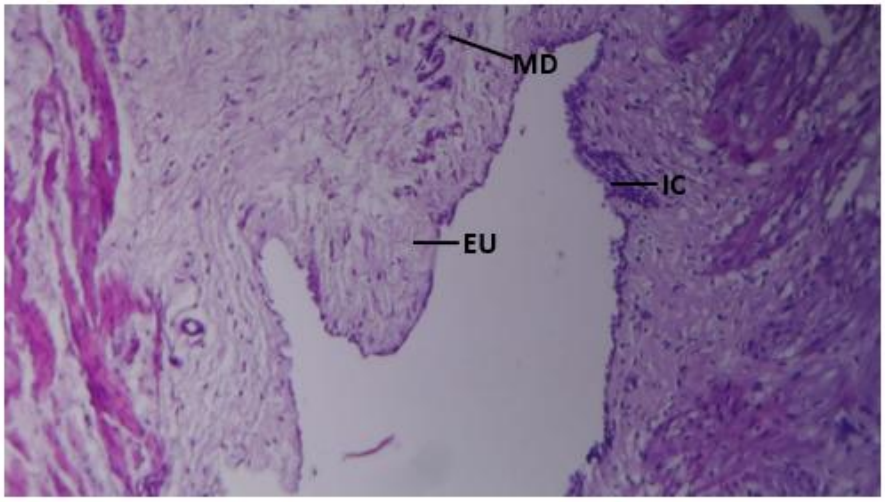

Plate 19. Group C: Histopathology micrograph of uterus of postpartum female wistar albino rats exposed to dimethoate showing: endometrial lining ulceration (EU), stromal myxoid degeneration (MD) and stromal infiltrates of inflammatory cells (IC): H&E 100 X

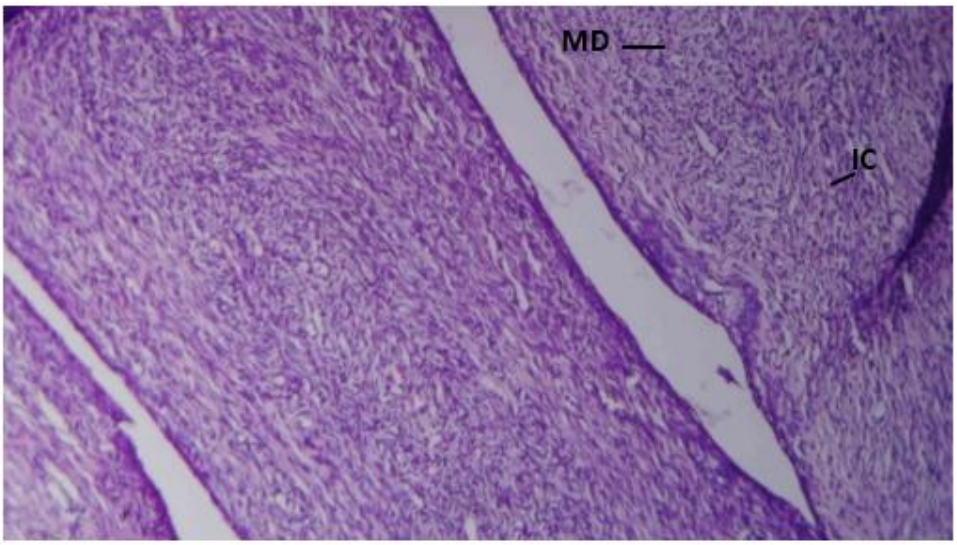

Plate 20. Group D: Histopathology micrograph of uterus of postpartum female wistar albino rats exposed to cypermethrin showing: stromal myxoid degeneration (MD) and stromal infiltrates of inflammatory cells (IC): H&E 100 X

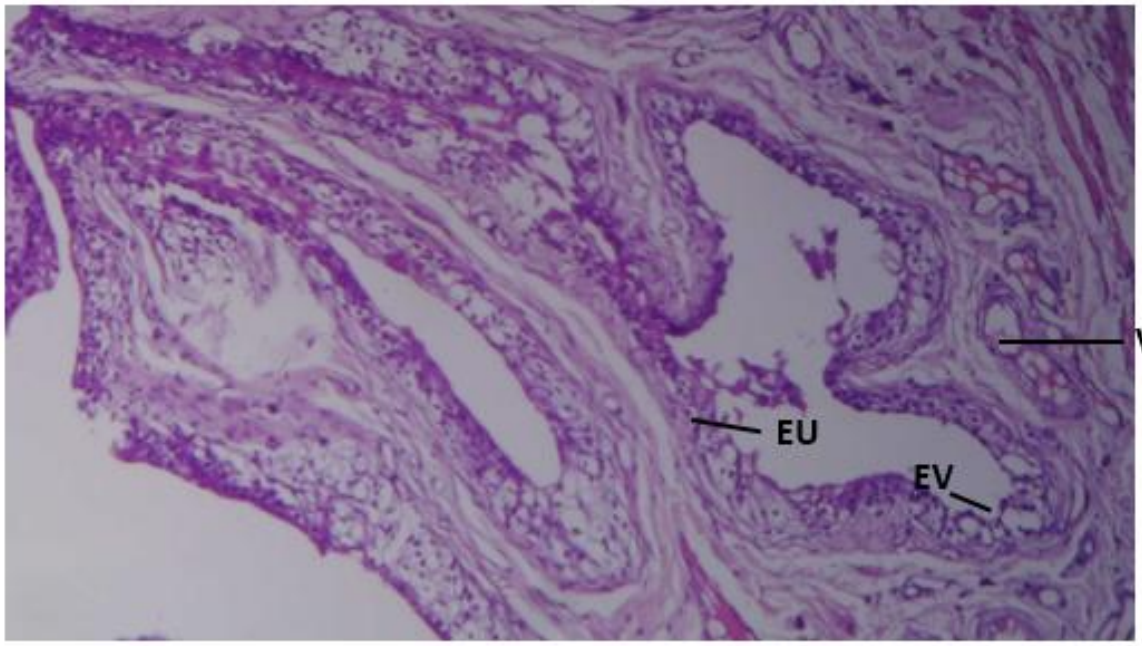

Plate 21. Group E: Histopathology micrograph of uterus of postpartum female wistar albino rats exposed to dichlorvos and dimethoate showing: endometrial lining ulceration (EU), endometrial lining epithelial vacuolation (EV) and stromal vascular degeneration (VD): H&E 100 X

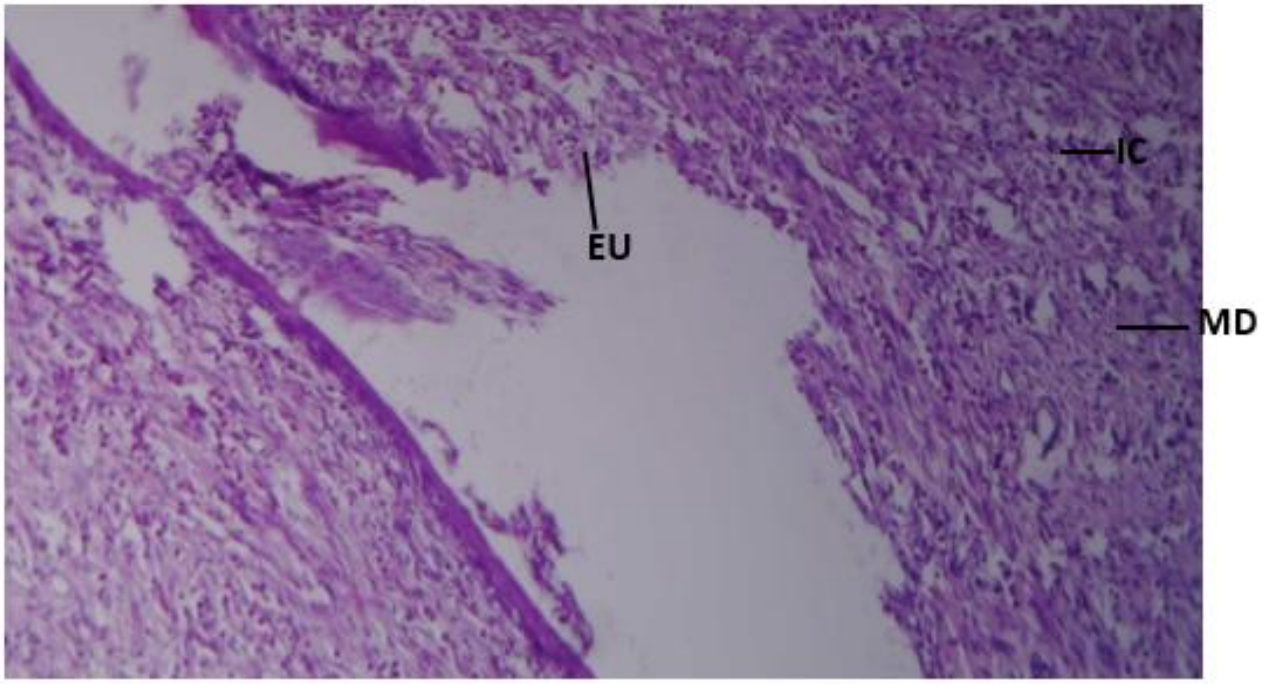

Plate 22. Group F: Histopathology micrograph of uterus of postpartum female wistar albino rats exposed to dichlorvos and cypermethrin showing severe endometrial lining ulceration (EU), endometrial stromal myxoid degeneration (MD) and stromal infiltrates of inflammatory cells (IC): H&E 100 X

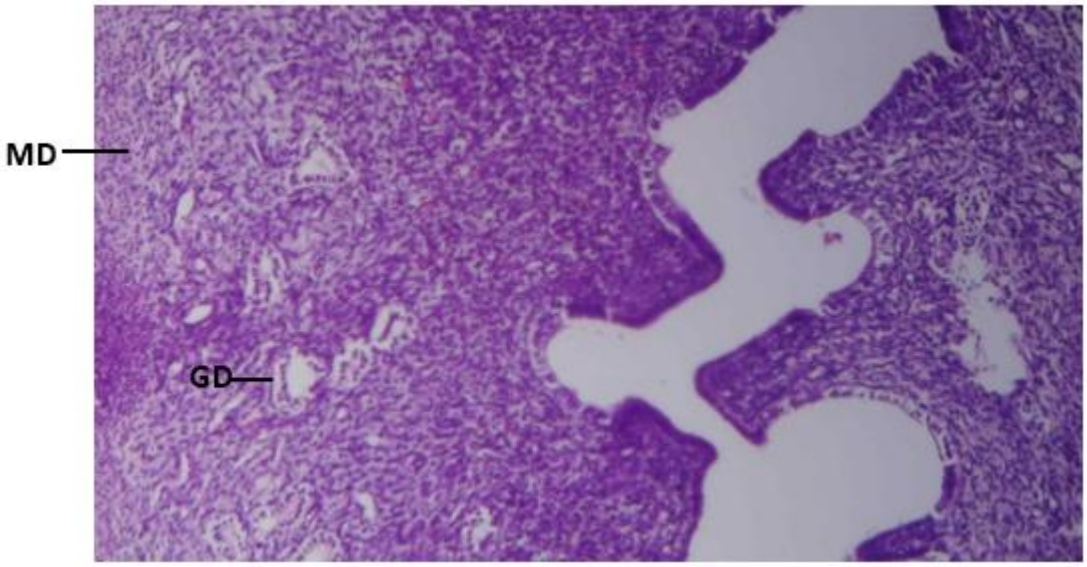

Plate 23. Group G: Histopathology micrograph of uterus of postpartum female wistar albino rats exposed to dimethoate and cypermethrin showing endometrial stromal myxoid degeneration (MD) and severe endometrial glandular degeneration (GD): H&E 100 X

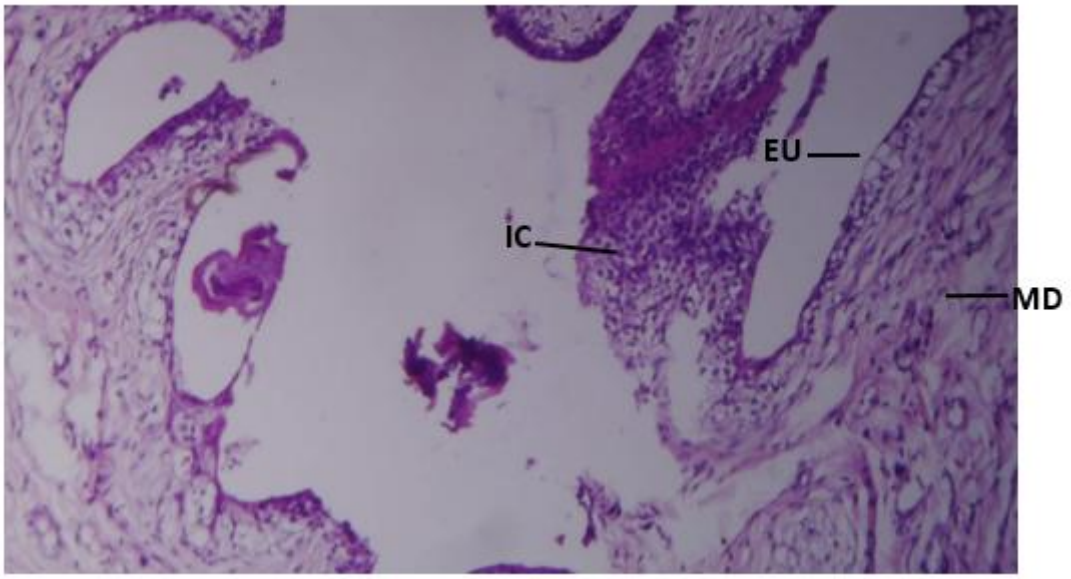

Plate 24. Group H: Histopathology micrograph of uterus of postpartum female wistar albino rats exposed to dichlorvos, dimethoate, and cypermethrin showing severe endometrial lining vacuolation (EV), heavy stromal infiltrates of inflammatory cells (IC) and stromal myxoid degeneration (MD): H&E 100 X

The histopathology micrographs in plates 25 to 32 illustrate the ovarian tissue of postpartum female Wistar albino rats subjected to different pesticide exposures. The effects on follicle viability, stromal condition, and overall ovarian architecture vary with each pesticide and combination, revealing insights into the toxicological impact on ovarian health. Below is a comprehensive interpretation of each plate.

Plate 25 (Group A): This control image represents the ovary of rats exposed only to sprayed water. It shows normal ovarian architecture with follicles (FO) at various developmental stages, four of which are viable. The stroma (ST) is vascularized, providing adequate support for follicle development, and the coelomic epithelium (CE) appears intact. This normal structure serves as a reference to identify the impact of pesticide exposure in the other groups.

Plate 26 (Group B): In the ovary of rats exposed to dichlorvos, maturing follicles (FO) are evident, with four viable follicles present. The stroma has become luteinized (ST), and a corpus luteum (CL) is also visible. The luteinization of the stroma might indicate early hormonal effects of dichlorvos exposure, which could alter the normal reproductive cycle by influencing the structural and functional aspects of the ovary.

Plate 27 (Group C): The ovarian tissue of rats exposed to dimethoate displays both developing (FO) and degenerating follicles (DF), with severe stromal congestion (SC) present. While four follicles remain viable, the degeneration of others suggests that dimethoate may induce follicular atresia, with congestion in the stroma further indicating compromised vascular support that could impact follicle viability.

Plate 28 (Group D): In this group, where rats were exposed to cypermethrin, the ovary shows maturing follicles (FO), with only two viable follicles present alongside degenerating follicles (DF). The supporting stroma is luteinized (ST). The reduced number of viable follicles combined with degenerative changes suggests that cypermethrin may disrupt follicle maturation and viability, potentially influencing reproductive function through stromal alterations.

Plate 29 (Group E): In the ovarian tissue of rats exposed to a combination of dichlorvos and dimethoate, only one viable follicle (FO) is observed, with several degenerating follicles (DF) present. The stroma has undergone luteinization (ST). The diminished number of viable follicles and increased degeneration indicate a cumulative toxic effect of these pesticides, suggesting that the combined exposure severely impacts follicular health and ovarian function.

Plate 30 (Group F): In this group, where dichlorvos and cypermethrin were combined, the ovary contains follicles in early development stages (FO), with four viable follicles supported by a luteinized stroma (ST). The relative preservation of follicle viability, despite stromal luteinization, suggests that this combination may be less detrimental to follicle health compared to other pesticide combinations. However, the luteinization of the stroma could still indicate potential hormonal or structural alterations.

Plate 31 (Group G): The ovary of rats exposed to dimethoate and cypermethrin shows five viable maturing follicles (FO), supported by a luteinized stroma (ST). The presence of multiple viable follicles suggests that this combination may have a relatively milder impact on follicle viability, though the luteinization of the stroma could signify underlying alterations in ovarian structure and function.

Plate 32 (Group H): The combined exposure to dichlorvos, dimethoate, and cypermethrin results in the ovary containing only one viable developing follicle (FO) amidst degenerating follicles (DF). The supporting stroma is luteinized (ST). The limited number of viable follicles, along with extensive degeneration, reflects the severe cumulative toxic effect of the three pesticides, indicating substantial disruption to ovarian health and reproductive potential.

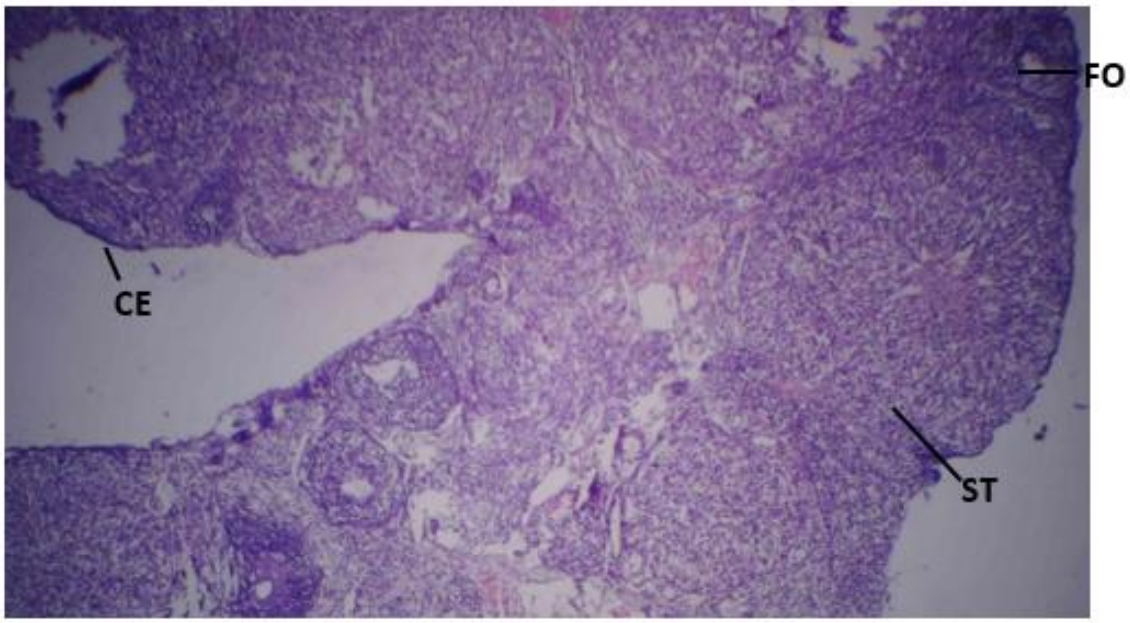

Plate 25. Group A: Histopathology micrograph of ovary of postpartum female wistar albino rats exposed to sprayed water showing follicles (FO) in various developmental stages-4 viable, supported by a vascularized stroma (ST), coelomic epithelium (CE): H&E 40 X

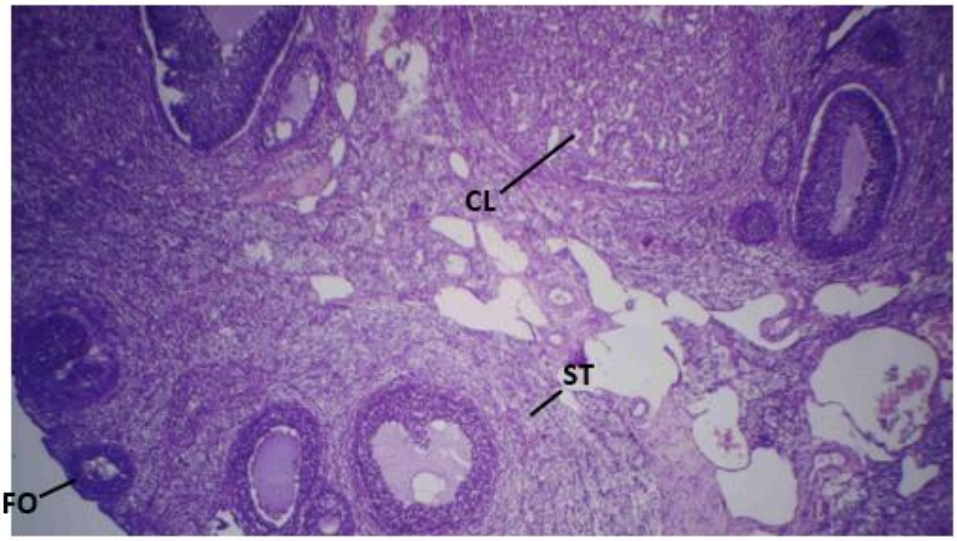

Plate 26. Group B: Histopathology micrograph of ovary of postpartum female wistar albino rats exposed to dichlorvos showing: maturing follicles (FO) – 4 viable, supported by a luteinized stroma (ST), corpus luteum (CL): H&E 40 X

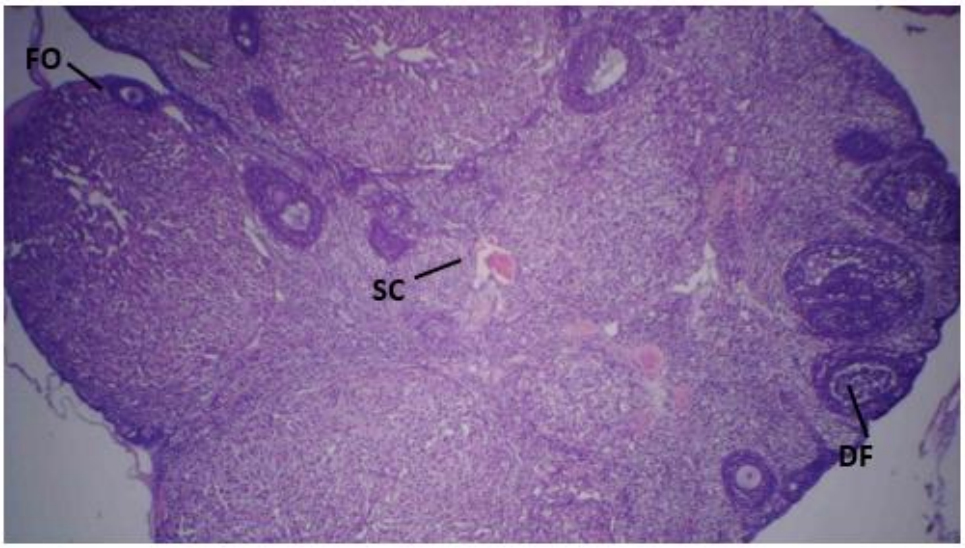

Plate 27. Group C: Histopathology micrograph of ovary of postpartum female wistar albino rats exposed to dimethoate showing: developing follicles (FO) – 4 viable, degenerating follicles (DF), severe stromal congestion (SC): H&E 40 X

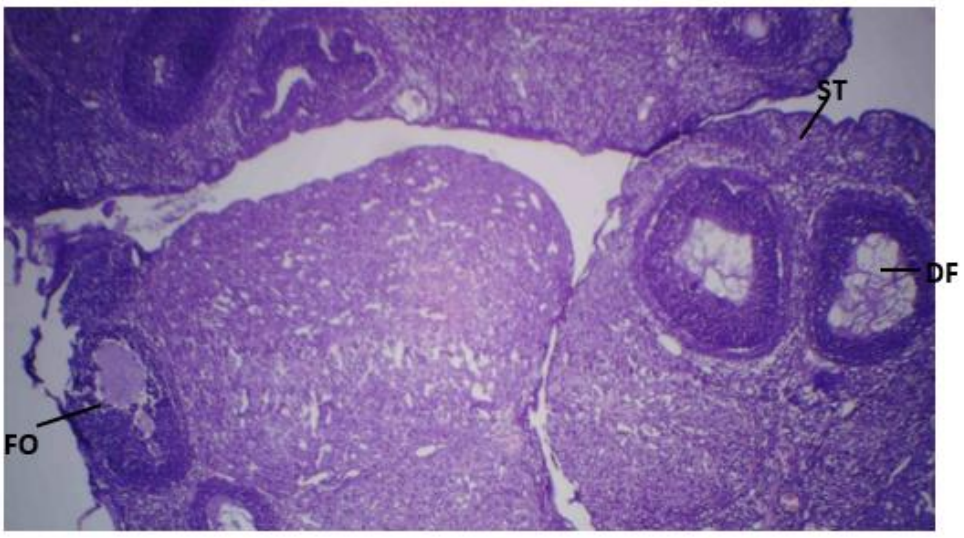

Plate 28. Group D: Histopathology micrograph of ovary of postpartum female wistar albino rats exposed to cypermethrin showing: maturing follicles (FO) – 2 viable, degenerating follicles (DF), supported by a luteinized stroma (ST): H&E 40 X

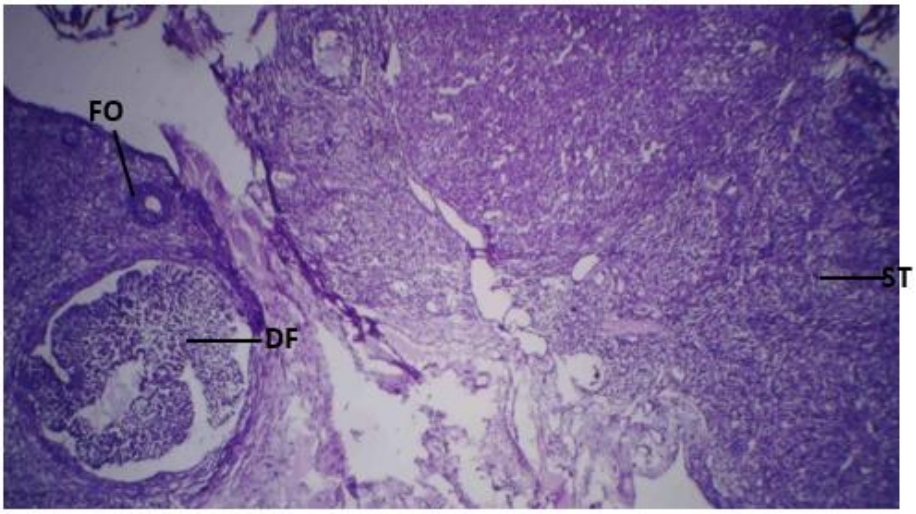

Plate 29. Group E: Histopathology micrograph of ovary of postpartum female wistar albino rats exposed to dichlorvos and dimethoate showing developing follicles (FO) – 1 viable, degenerating follicles (DF), supported by a luteinized stroma (ST): H&E 40 X

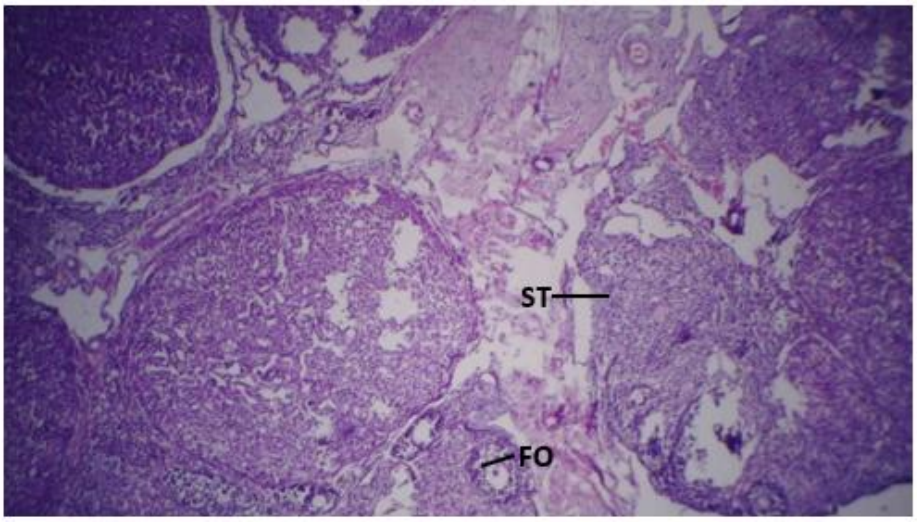

Plate 30. Group F: Histopathology micrograph of ovary of postpartum female wistar albino rats exposed to dichlorvos and cypermethrin showing follicles in early stages of development (FO) – 4 viable supported by a luteinized stroma (ST): H&E 40 X

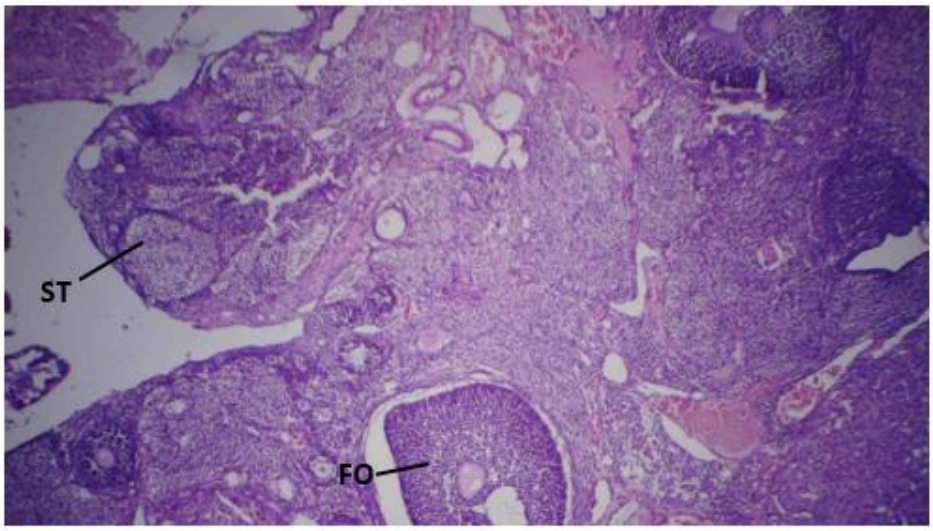

Plate 31. Group G: Histopathology micrograph of ovary of postpartum female wistar albino rats exposed to dimethoate and cypermethrin showing maturingfollicles (FO) – 5 viable supported by a luteinized stroma (ST): H&E 40 X

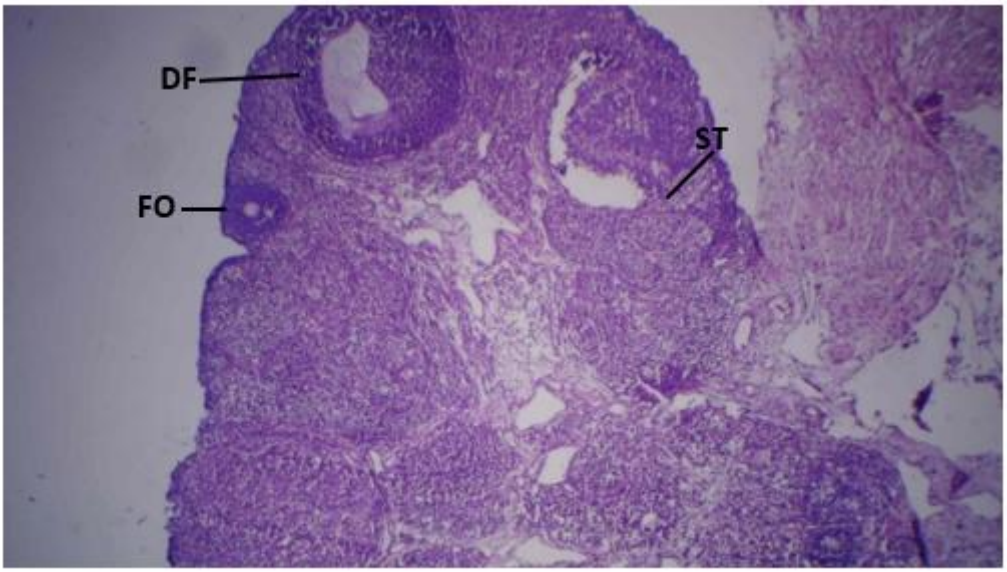

Plate 32. Group H: Histopathology micrograph of ovary of postpartum female wistar albino rats exposed to dichlorvos, dimethoate, and cypermethrin showing developing follicles (FO) – 1 viable, degenerating follicles (DF), supported by luteinized stroma (ST): H&E 40 X

DISCUSSION

Haematological Impacts

The analysis of RBC, hemoglobin (HB), and platelet counts in both female and postpartum Wistar rats indicated marked hematotoxic effects. RBC and HB levels showed significant reductions in groups exposed to Dichlorvos (Group B) and its combinations with Dimethoate and Cypermethrin, with postpartum rats exhibiting slightly higher resilience compared to non-postpartum females. Platelet counts increased significantly in the pesticide-exposed groups, reflecting a compensatory mechanism possibly linked to bone marrow stimulation or systemic inflammatory responses.

The observed decline in RBC and HB aligns with previous studies, such as Manna et al. (2004), who reported a reduction in these parameters following exposure to Cypermethrin. This effect is attributed to oxidative damage to erythrocyte membranes, leading to hemolysis (Manna et al., 2004). Similarly, Çelik et al. (2009) found that sublethal doses of Dichlorvos caused leukocytosis and disrupted hematocrit levels, suggesting systemic stress and marrow compensatory mechanisms (Çelik et al., 2009).

Additionally, the platelet elevation observed in this study can be linked to the systemic inflammatory response and bone marrow hyperplasia noted in pesticide-exposed rats. Aroonvilairat et al. (2018) reported similar findings, where exposure to Cypermethrin and other pesticides induced leukocytosis and elevated platelets, highlighting a compensatory response to pesticide-induced toxicity (Aroonvilairat et al., 2018).

The enhanced resilience in postpartum rats may reflect adaptive physiological mechanisms, such as heightened erythropoietic responses during postpartum recovery. This finding necessitates further investigation into the protective roles of postpartum physiology in mitigating hematotoxicity. The haematological alterations underscore the potential risks associated with pesticide exposure, particularly in reproductive contexts. These findings are consistent with existing literature, reinforcing the detrimental impact of pesticides on blood parameters. Future research should delve deeper into the mechanisms of hematotoxicity and explore strategies for mitigating such effects in exposed populations.

In terms of hematological resilience, the ability of postpartum rats to maintain higher RBC and hemoglobin levels compared to non-postpartum females could be linked to enhanced erythropoietic activity post-delivery. Aroonvilairat et al. (2018) noted that adaptive responses to systemic stress, such as increased bone marrow activity, are more pronounced in reproductive stages like lactation, potentially explaining the observed differences (Aroonvilairat et al., 2018).

Histopathological Evidence

Histopathological analysis revealed significant tissue damage in reproductive organs, including the ovaries and uterus, across pesticide-exposed groups. Key findings included degenerative changes in ovarian follicles, disrupted uterine architecture, and inflammatory cell infiltration. The severity was highest in rats exposed to Dichlorvos, Dimethoate, and Cypermethrin mixtures (Group E), with postpartum rats showing comparatively less pronounced damage than non-postpartum females.

The structural and cellular damage observed in ovarian and uterine tissues aligns with the documented effects of pesticide exposure in rodent models. Cypermethrin has been reported to induce histopathological changes such as follicular atresia, stromal edema, and ovarian degeneration due to oxidative stress and disrupted steroidogenesis. For instance, Shuklan et

al. (2023) found significant histopathological changes in the ovaries and uterus of Cypermethrin-exposed rats, including hemorrhage and cellular necrosis (Shuklan et al., 2023).

Dichlorvos and Dimethoate exposure has also been implicated in inducing structural damage to reproductive organs. Wang et al. (2013) reported degenerative changes in ovarian and uterine tissues, attributing these effects to oxidative damage and impaired cellular repair mechanisms (Wang et al., 2013). Furthermore, Nehéz et al. (1994) highlighted chromosomal aberrations and cellular damage in bone marrow and reproductive tissues following Dichlorvos and Dimethoate exposure, consistent with the findings of this study (Nehéz et al., 1994).

The histopathological damage was most pronounced in groups exposed to combined pesticide treatments, indicating potential synergistic effects. This observation corroborates studies such as those by Lengyel et al. (2007), who found amplified histological changes in reproductive tissues following combined pesticide exposure. The mechanism likely involves cumulative oxidative stress, inflammation, and direct cellular toxicity (Lengyel et al., 2007).

Postpartum rats exhibited comparatively less severe histopathological damage, suggesting protective physiological adaptations. Elevated levels of antioxidants and hormonal fluctuations during the postpartum period may confer resistance against pesticide-induced tissue damage. This observation aligns with Rashid et al. (2022), who suggested that postpartum hormonal adaptations could mitigate some oxidative and inflammatory effects of toxicants (Rashid et al., 2022).

The structural damage to ovarian and uterine tissues poses significant risks to fertility and reproductive function. Follicular degeneration and uterine inflammation may impair ovulation, implantation, and pregnancy maintenance, with potential long-term reproductive consequences. These findings emphasize the need to address combined pesticide exposures, particularly in vulnerable populations such as pregnant and postpartum females.

The histopathological evidence from this study highlights the severe impact of pesticide exposure on reproductive tissues, particularly under combined exposure conditions. Postpartum resilience offers valuable insights for future research, potentially guiding protective interventions. These findings underline the importance of regulating pesticide use and advancing studies on tissue-specific toxicity mechanisms.

CONFLICT OF INTEREST

The authors declare no conflict of interest regarding the publication of this study.

REFERENCES

I. Aroonvilairat, S., Tangjarukij, C., Sornprachum, T., Chaisuriya, P., Siwadune, T., & Ratanabanangkoon, K. (2018). Effects of topical exposure to a mixture of chlorpyrifos, cypermethrin and captan on the hematological and immunological systems in male Wistar rats. *Environmental Toxicology and Pharmacology, 59,* 53-60. https://doi.org/10.1016/j.etap.2018.02.010

II. Bouabdallah, I., Boukhris, I., & Hamden, K. (2022). Toxic impacts of a mixture of three pesticides on the reproduction and fertility of male rats. *Journal of Advanced Biotechnology and Bioengineering*, 10(1), 1-10.

III. Celik, I., Yilmaz, Z., & Turkoglu, V. (2009). Hematotoxic and hepatotoxic effects of dichlorvos at sublethal dosages in rats. *Environmental Toxicology*, 24(2), 128-132.

IV. Drury, R.A.B and Wallington, E.A. (1973). Tissue histology. In: Carleton's Histological Technique 4th ed. Oxford University press, New York. Pp 58.

V. Gupta, R. C., Milatovic, D., & Dettbarn, W. D. (2021). Pyrethroid insecticides: poisoning syndromes, synergies, and therapies. *Toxicology and Applied Pharmacology*, 429, 115683.

VI. Hart, J. S., & Ibeachu, P. C. (2022). Histological changes in rat testicular tissue architecture upon short-term exposure to inhaled dichlorvos. *School Bulletin*, 8(4), 111-114.

VII. Kumar, S. V., Fareedullah, M. D., Sudhakar, Y., Venkateswarlu, B., & Kumar, E. A. (2010). Current review on organophosphorus poisoning. *Archives of Applied Science Research*, 2(4), 199-215.

VIII. Lengyel, Z., Fazakas, Z., & Nagymajtényi, L. (2005). Changes in the central nervous activity of rats treated with dimethoate in combination with other neurotoxicants in different phases of ontogenesis. *Arhiv za Higijenu Rada i Toksikologiju, 56(3),* 257-264. https://consensus.app/papers/changes-activity-rats-treated-combination-lengyel/8ca7d32ddcc75f138e18652271aa9223/

IX. Manna, S., Bhattacharyya, D., Mandal, T., & Das, S. (2004). Repeated dose toxicity of alpha-cypermethrin in rats. *Journal of Veterinary Science, 5(3),* 241-245. https://doi.org/10.4142/JVS.2004.5.

X. Mitruka, B.M. and Rawnsley, .M. (1977). Materials and methods in hematology and clinical biochemistry. In: Clinical Biochemical and Hematological Reference Values in Normal Experimental Animals. Masson Publishing Inc. USA. Pp 41-58.

XI. Nehéz, M., Tóth, C., & Dési, I. (1994). The effect of dimethoate, dichlorvos, and parathion-methyl on bone marrow cell chromosomes of rats in subchronic experiments in vivo. *Ecotoxicology and Environmental Safety, 29(3),* 365-371. https://doi.org/10.1016/0147-6513(94)90009-4

XII. Rashid, U., Qureshi, I. Z., Jan, S., Khalid, T., & Khan, D. A. (2022). Preventive effects of selenium against cypermethrin-induced haematological toxicity in Sprague-Dawley rats. *World Journal of Biology Pharmacy and Health Sciences*, n.p. https://doi.org/10.30574/wjbphs.2022.12.1.0115

XIII. Shuklan, P., Raj, A., Chauhan, K., Madan, P., & Rani, S. (2023). Systematic toxicity of Cypermethrin and alterations in behavior of albino rats. *ACS Omega*, *8*, 14766-14773. https://doi.org/10.1021/acsomega.3c00817

XIV. Udodi, P. S., Anonye, T. C., & Ezejindu, D. N. (2023). Exposure to insecticide mixture of cypermethrin and dichlorvos induced neurodegeneration by reducing antioxidant capacity in striatum. *Journal of Chemical Health Risks*, 13(3), 211-220.

XV. Wang, Q., Zhang, Y.-J., Zhou, C.-X., Zhang, J., Dou, Y., & Li, Q. (2013). Risk assessment of mouse gastric tissue cancer induced by dichlorvos and dimethoate. *Oncology Letters*, *5*, 1385-1389. https://doi.org/10.3892/ol.2013.1155